






Research Article

Delimitation of the genus *Schizachyrium* (Poaceae, Andropogoneae) based on molecular and morphological data

Myriam C. Peichoto^{1,2*} , Ercilia M. S. Moreno³ , Cassiano A. D. Welker⁴ , Viviana G. Solís Neffa^{2,3} , and M. Amalia Scataglini⁵ 

¹Facultad de Ciencias Agrarias, Universidad Nacional del Nordeste, Sargento Cabral 2131, Corrientes 3400, Argentina

²Instituto de Botánica del Nordeste (UNNE-CONICET), Sargento Cabral 2131, Casilla de Correo 209, Corrientes 3400, Argentina

³Facultad de Ciencias Exactas y Naturales y Agrimensura, Universidad Nacional del Nordeste, Avenida Libertad 5470, Corrientes 3400, Argentina

⁴Instituto de Biología, Universidade Federal de Uberlândia, Rua Ceará s.n., Uberlândia, Minas Gerais 38400-902, Brazil

⁵Instituto de Botánica Darwinion (ANCEFN-CONICET), Labardén 200, Casilla de Correo 22, B1642HYD San Isidro, Buenos Aires, Argentina

*Author for correspondence. E-mail: cpeichoto@yahoo.com.ar

Received 27 April 2020; Accepted 17 July 2021; Article first published online 21 July 2021

Abstract *Schizachyrium* (Poaceae, Andropogoneae) includes about 60 species distributed in tropical and subtropical regions of the world. In all recent molecular phylogenies of Andropogoneae, representatives of *Schizachyrium* appear closely related to *Andropogon* species. The objective of this study was to contribute to the delimitation of *Schizachyrium*. We performed a phylogenetic study including 38 taxa (>63%) of *Schizachyrium*, along with representatives of related genera, mainly of *Andropogon*, yielding a total of 49 taxa. This is the first phylogenetic analysis to include the type species of *Schizachyrium*, *S. condensatum*. DNA sequences of two plastid markers (*ndhF* and *trnL-F*) were analyzed under Bayesian methods. The results indicate that *Schizachyrium* is not monophyletic: 26 of the 38 *Schizachyrium* taxa analyzed are placed in a *Schizachyrium* s.s. clade that includes the type species of the genus, while 10 taxa are related to *Andropogon* species and two other species, *S. delavayi* (from China and India) and *S. jeffreysii* (from Africa), appear clearly separated. Additionally, 58 morphological characters (41 qualitative and 17 quantitative) were scored for the same 49 taxa and analyzed under the parsimony criterion. Character optimizations showed that (i) the reduced pedicellate spikelets, (ii) with lower glume less than or equal to 0.5 mm wide, (iii) awned, and (iv) without lemma and palea support the *Schizachyrium* s.s. clade. We propose these four characters as diagnostic features for the delimitation of *Schizachyrium* s.s.

Key words: DASH clade, grasses, molecular phylogeny, morphological analysis, Panicoideae.

1 Introduction

The genus *Schizachyrium* Nees (Poaceae, Andropogoneae) comprises ca. 60 species distributed in tropical and subtropical regions of the world, mostly concentrated in America and Africa (Türpe, 1984; Clayton & Renvoize, 1986; Nicora & Rúgolo de Agrasar, 1987; Peichoto, 2010; Soreng et al., 2017), although both native and endemic species have also been described in Asia and Australia (Watson & Dallwitz, 1992; Clayton et al., 2006; Shouliang & Phillips, 2006). During the revision of the South American species of *Schizachyrium* performed by Peichoto (2010), two morphological groups based on inflorescence traits were defined. One of the groups includes taxa with sparsely branched inflorescences with one to a few racemes and straight and thick rachis internodes and pedicels, such as *S. brevifolium* (Sw.) Nees ex Buse and morphologically similar species. The other group comprises taxa with highly branched inflorescences and

flexuous and slender rachis internodes and pedicels, zigzagging at maturity (Peichoto et al., 2008; Peichoto, 2010); this group includes the type species, *S. condensatum* (Kunth) Nees. Although most authors have considered *S. brevifolium* as the type of *Schizachyrium* (e.g., Clayton & Renvoize, 1986; Peichoto, 2010; Arthan et al., 2017), a recent investigation carried out by Welker et al. (2021) confirmed that *S. condensatum* is the correct type of the genus. Whether these two morphological groups are monophyletic or not is not known since it has not been tested using molecular markers on a large representative sample.

Schizachyrium is morphologically similar to *Andropogon* L. (the type genus of the tribe Andropogoneae), which includes ca. 120 species mainly from tropical and warm-temperate regions of the world, with a higher diversity in America and Africa (Clayton et al., 2006; Zanin & Longhi-Wagner, 2011; Soreng et al., 2017; Zannin et al., 2019). *Andropogon* has no obvious morphological synapomorphies that characterize the

genus (Arthan et al., 2017). Clayton (1964) mentioned that single racemes are probably of value in segregating *Schizachyrium* and recognized two sections; however, the feature number of racemes was never suggested as having generic significance for *Andropogon*, and more reliable characters can be found in the lower glume of the sessile spikelets, the rachis internodes, and the pedicels. A few species of *Andropogon* (e.g., *A. fastigiatus* Sw., *A. crucianus* Renvoize) have solitary racemes as in *Schizachyrium* (Zanin & Longhi-Wagner, 2011). Furthermore, among other characters that overlap in both genera, the pedicellate spikelets can be neutral or staminate (Clayton et al., 2006; Arthan et al., 2017). Species of *Andropogon* and *Schizachyrium* appear closely related in molecular phylogenies of Andropogoneae (e.g., Mathews et al., 2002; Skendzic et al., 2007; Teerawatananon et al., 2011; Estep et al., 2014; Arthan et al., 2017; McAllister et al., 2018; Welker et al., 2020). However, none of the molecular phylogenies carried out so far has included a large representative number of species of these two genera.

The phylogeny of the tribe Andropogoneae, which is a monophyletic group within the subfamily Panicoideae and includes ca. 1224 species distributed in 92 tropical and subtropical genera (Welker et al., 2020), has been difficult to resolve, especially because of polyploidy, reticulate evolution, and apparent rapid radiation early in the evolution of the tribe (Mathews et al., 2002; Skendzic et al., 2007; Bouchenak-Khelladi et al., 2008; Estep et al., 2014; Arthan et al., 2017). Based on the phylogenetic analysis of nuclear ribosomal internal transcribed spacer (ITS) and plastid intergenic spacer *trnL-F*, Skendzic et al. (2007) postulated that *Andropogon* (with five species analyzed) and *Schizachyrium* (nine species analyzed) were not monophyletic since their species appeared intermixed and related to *Hyparrhenia* Andersson ex E. Fourn. (one species analyzed). Teerawatananon et al. (2011) corroborated the close relationship between species of *Andropogon*, *Schizachyrium*, and *Hyparrhenia*, including two representatives of each genus. The genus *Hyparrhenia* includes ca. 60 species, distributed mainly in Africa and with a few species extending to other tropical regions (Clayton & Renvoize, 1986; Shouliang & Phillips, 2006; Soreng et al., 2017).

In their studies on allopolyploidy by using multiple low-copy nuclear genes, Estep et al. (2014) recovered a clade containing *Diheteropogon* (Hack.) Stapf (a small genus with ca. four African species; Soreng et al., 2017), *Andropogon*, *Schizachyrium*, and *Hyparrhenia*, which they named “DASH” clade, later called Andropogoninae sensu Soreng et al., (2015). Later, two plastome phylogenomic studies of Andropogoneae (Arthan et al., 2017; McAllister et al., 2018) have shed some light on these issues. Arthan et al. (2017) presented a plastome analysis, including 52 species (32 genera) from mainland Southeast Asia. The species sampled included five species of *Andropogon*, seven of *Schizachyrium*, and two of *Hyparrhenia* (but no sample of *Diheteropogon*). The DASH clade (including only *Andropogon*, *Schizachyrium*, and *Hyparrhenia*) displayed four internal clades: (i) a clade composed of *Hyparrhenia* and some species of *Andropogon*, (ii) an *Andropogon-Schizachyrium* mixed clade (including *S. tenerum* Nees and *S. imberbe* A. Camus), (iii) a clade formed by the specimens of *Andropogon chinensis* (Nees) Merr. sampled, and (iv) an exclusive *Schizachyrium* clade, including

S. brevifolium and related species (Arthan et al., 2017). McAllister et al. (2018) conducted a specimen-based analysis of morphology and the environment together with a plastome analysis of the tribe Andropogoneae, including plastome sequences of 14 *Schizachyrium* species. Similarly to that found by Arthan et al. (2017), these authors obtained an exclusive *Schizachyrium* clade (called *Schizachyrium* s.s. clade), a clade with *Andropogon* species of the sections *Notosolen* Stapf and *Piestium* Stapf (including *A. chinensis*), and an *Andropogon-Schizachyrium* mixed clade called “Dietomis” clade (McAllister et al., 2018). The remaining species of *Andropogon* sampled were recovered in several other clades in the plastome tree of McAllister et al. (2018). More recently, Welker et al. (2020) performed a plastome phylogenomic analysis of Andropogoneae with the largest sample of the tribe to date (67 genera and 204 species) and confirmed that the genera *Andropogon* (with 38 species analyzed) and *Schizachyrium* (18 species analyzed) are polyphyletic, similarly to the previous works mentioned above.

It is clear that the complexity of the relationships between *Schizachyrium* and *Andropogon* is a subject in which much remains to be done. Since none of the studies described above has sampled the genus *Schizachyrium* in depth or included its correct type (*S. condensatum*), our objective is to focus on moving toward the circumscription of the genus, increasing the species sampling with the type species. The aim of the present work was to perform a molecular and morphological phylogenetic study analyzing a broad sampling of *Schizachyrium*, focused not only on American species but also covering the entire distributional range of the genus, to circumscribe the *Schizachyrium* s.s. clade, analyze infrageneric groups, and improve upon the known phylogeny among species related to *Andropogon*.

2 Material and Methods

2.1 Taxon sampling

Forty-nine taxa were included in the molecular and morphological analyses. Thirty-eight of these taxa belong to *Schizachyrium* (23 from America, 7 from Africa, 1 from Asia, 1 from Australia, 2 from Asia and Australia, 1 from Africa and America, 1 from Africa and Asia, and 2 with wide distribution), whereas 7 belong to *Andropogon* [*A. chinensis*, *A. distachyos* L., *A. fastigiatus*, *A. gayanus* Kunth, *A. gerardi* Vitman, *A. glomeratus* (Walter) Britton, Sterns & Poggenb., and *A. ternarius* Michx.]. One representative of each of the following related genera was also included: *Cymbopogon citratus* (DC.) Stapf, *Dichanthium aristatum* (Poir.) C.E. Hubb., and *Hyparrhenia rufa* (Nees) Stapf. *Bothriochloa bladhii* (Retz.) S.T. Blake was used to root the trees based on Skendzic et al. (2007). Details of all taxa analyzed, including the authors of scientific names, are listed in Table 1.

2.2 Molecular data

Sequences of *Andropogon* and other Andropogoneae genera were obtained from GenBank based on previous works (Spangler et al., 1999; Skendzic et al., 2007; Bouchenak-Khelladi et al., 2009; Teerawatananon et al., 2011; Preston

Table 1 List of *Schizachyrium* taxa and relatives analyzed and GenBank accession numbers

Species	Voucher	GenBank accession No.	
		<i>ndhF</i>	<i>trnL-trnF</i>
<i>Andropogon chinensis</i> (Nees) Merr.		HM346963 (Bouchenak-Khelladi et al., 2014)	KY596121 (Arthan et al., 2017)
<i>A. distachyos</i> L.		KY596170 (Arthan et al., 2017)	DQ004951 (Skendzic et al., 2007)
<i>A. fastigiatus</i> Sw.		KY596180 (Arthan et al., 2017)	DQ004977 (Skendzic et al., 2007)
<i>A. gayanus</i> Kunth		JN560735 (Preston et al., 2012)	MH181211 (McAllister et al., 2018)
<i>A. gerardii</i> Vitman		AF117391 (Spangler et al., 1999)	DQ004952 (Skendzic et al., 2007)
<i>A. glomeratus</i> (Walter) Britton, Sterns & Poggenb.		–	DQ004953 (Skendzic et al., 2007)
<i>A. ternarius</i> Michx.		–	DQ004954 (Skendzic et al., 2007)
<i>Bothriochloa bladhii</i> (Retz.) S.T. Blake		AF117395 (Spangler et al., 1999)	DQ004960 (Skendzic et al., 2007)
<i>Cymbopogon citratus</i> (DC.) Stapf		MF998615 (Hackel et al., 2018)	EF137581 (Bouchenak-Khelladi et al., 2009)
<i>Dichanthium aristatum</i> (Poir.) C.E. Hubb.		AF117409 (Spangler et al., 1999)	–
<i>Hyparrhenia rufa</i> (Nees) Stapf		–	GQ869964 (Teerawatananon et al., 2011)
<i>Schizachyrium bimucronatum</i> Roseng., B. R. Arrill. & Izag.	Peichoto 138 (CTES), Argentina	MW220955	MW220992
<i>S. brevifolium</i> (Sw.) Nees ex Buse	Johnston 934 (GH), Panama	MW220956	MW220993
<i>S. cirratum</i> (Hack.) Nash	Makings 3035 (CTES), U.S.A.	MW220957	DQ004990 (Skendzic et al., 2007)
<i>S. condensatum</i> (Kunth) Nees	Peichoto 54 (CTES), Argentina	MW220958	MW220994
<i>S. cubense</i> (Hack.) Nash	León 17886 (GH), Cuba	MW220959	MW220995
<i>S. delavayi</i> (Hack.) Bor	Boufford 37873 (MO), China	MW220960	MW220996
<i>S. exile</i> (Hochst.) Pilg.	Raltea 1797 (A), Africa	MW220961	–
<i>S. fragile</i> (R.Br.) A. Camus	Fosberg 35432 (US), Guam (Marianas Islands)	MW220962	MW220997
<i>S. glaziovii</i> Peichoto	Peichoto 169 (CTES), Argentina	MW220963	MW220998
<i>S. gracilipes</i> (Hack.) A. Camus	Peichoto 122 (CTES), Paraguay	MW220964	MW220999
<i>S. hatschbachii</i> Peichoto	Peichoto 131 (CTES), Argentina	MW220965	MW221000
<i>S. imberbe</i> A. Camus	Peichoto 236 (CTES), Argentina	MW220966	MW221001
<i>S. jeffreysii</i> (Hack.) Stapf	Bingham 274 (MO), Zimbabwe	MW220967	MW221002
<i>S. lactiflorum</i> (Hack.) Herter	Peichoto 232 (CTES), Argentina	MW220968	MW221003
<i>S. lomaense</i> A. Camus	Adam 24096 (MO), Australia	MW220969	MW221004
<i>S. maclaudii</i> (Jacq.-Fél.) S.T. Blake	Swallen 4514 (MO), Brazil	MW220970	MW221005
<i>S. malacostachyum</i> (J. Presl) Nash	Hitchcock 23225 (US), Mexico	MW220971	MW221006
<i>S. maritimum</i> (Chapm.) Nash	Godfrey 52658 (GH), USA	MW220972	MW221007

Continued

Table 1 Continued

Species	Voucher	GenBank accession No.	
		<i>ndhF</i>	<i>trnL-trnF</i>
<i>S. microstachyum</i> (Desv. ex Ham.) Roseng., B.R. Arrill. & Izag.	Peichoto 82 (CTES), Argentina	MW220973	MW221008
<i>S. multinervosum</i> Nash	León 6326 (US), Cuba	MW220974	MW221009
<i>S. mukuluense</i> Vanderyst	Corby 154 (US), Zimbabwe	MW220975	MW221010
<i>S. nodulosum</i> (Hack.) Stapf	Sihvonen 263 (US), Africa	MW220976	MW221011
<i>S. pachyarthron</i> C.A. Gardner	Lazarides 8891 (CANB), Australia	MW220977	MW221012
<i>S. paucispiculatum</i> Sulekic & Peichoto	Peichoto 167 (CTES), Argentina	MW220978	MW221013
<i>S. platyphyllum</i> (Franch.) Stapf	Kayombo 2753 (MO), Tanzania	MW220979	MW221014
<i>S. plumigerum</i> (Ekman) Parodi	Peichoto 171 (CTES), Argentina	MW220980	MW221015
<i>S. pseudolalia</i> (Hosok.) S.T. Blake	Simon 2677 (CANB), Australia	MW220981	MW221016
<i>S. rhizomatum</i> (Swallen) Gould	Killip 42266 (US), USA	MW220982	MW221017
<i>S. rupestre</i> (K. Schum.) Stapf	Fay 6522 (MO), Central African Republic	MW220983	MW221018
<i>S. sanguineum</i> (Retz.) Alston	Peichoto 154 (CTES), Argentina	MW220984	MW221019
<i>S. scabriflorum</i> (Rupr. ex Hack.) A. Camus	Peichoto 147 (CTES), Argentina	MW220985	MW221020
<i>S. schweinfurthii</i> (Hack.) Stapf	Rose-Innes 30439 (US), Ghana	MW220986	MW221021
<i>S. scoparium</i> (Michx.) Nash var. <i>scoparium</i>	Franklin 2406 (GH), USA	MW220987	MW221022
<i>S. scoparium</i> var. <i>neomexicanum</i> (Nash) Hitchc.	Moore & Steyermark 3369 (US), U.S.A.	MW220988	DQ004992 (Skendzic et al., 2007)
<i>S. scoparium</i> var. <i>stoloniferum</i> (Nash) Wipff	Kral 90492 (GH), USA	MW220989	MW221023
<i>S. semitectum</i> (Swallen) Reeder		-	DQ004996 (Skendzic et al., 2007)
<i>S. spicatum</i> (Spreng.) Herter	Peichoto 240 (CTES), Argentina	MW220990	MW221024
<i>S. tenerum</i> Nees	Peichoto 164 (CTES), Argentina	MW220991	MW221025

New sequences are highlighted in bold (MW220955–MW221025) and their voucher information is given. Literature references are provided for sequences from previous works.

et al., 2012; Bouchenak-Khelladi et al., 2014; Arthan et al., 2017; Hackel et al., 2018; McAllister et al., 2018).

Fresh leaves of 14 species collected directly from nature or derived from seeds grown in the laboratory were stored in silica gel. Total genomic DNA of these 14 species was extracted using the CTAB procedure of Doyle & Doyle (1987). DNA from herbarium material of 24 samples was obtained using a DNeasy Plant Mini Kit (QIAGEN Inc., Hilden, Germany). The complete *ndhF* gene and the plastid intergenic spacer *trnL-F* were amplified for the *Schizachyrium* samples. For *ndhF* amplification, the following pairs of primers specified by Olmstead & Sweere (1994) were used: 5F-536R, 536F-972F, 972F-1666R, and 1666F-3R. For *trnL-F* amplification, we used the pairs of primers c-d and e-f from Taberlet et al. (1991). PCR reactions were performed in a 25 µl final volume with 50–100 ng of template DNA, 0.2 µM

of each primer, 25 µM of each dNTP, 5 mM MgCl₂, 1× buffer and 1.5 units of Taq polymerase. The reaction conditions were: denaturation at 94 °C for 5 min, followed by 35 cycles of denaturation at 94 °C for 30 sec, annealing at 48 °C for 1 min, and extension at 72 °C for 1 min. The reactions were terminated by means of a final extension at 72 °C for 6 min. Negative control with no template was included for each series of amplification to eliminate the possibility of contamination. Amplifications were confirmed by electrophoresis in 1% TBE agarose gels stained with SYBR Safe (Invitrogen). Automated sequencing was performed by Macrogen Inc. (Seoul, Korea). Sequences were visually assessed and aligned with Bioedit v.5.0.9 (Hall, 1999). The 71 new sequences obtained were submitted to GenBank, with accessions numbers MW220955–MW221025 (see Table 1). The combined molecular matrix, including the

two plastid markers concatenated, is shown in Supplementary Material I.

2.3 Morphological data

The morphological matrix was constructed including the same 49 taxa of the molecular matrix. The list of material examined for morphological studies is shown in Supplementary Material II, based on herbarium collections from the following herbaria: CANB, CTES, F, G, GH, MO, NY, P, and US (herbarium acronyms according to Thiers, 2020). The morphological characters for the South American species of *Schizachyrium* were recorded from the descriptions of Peichoto (2010). For extra-American species, information was taken from the revision of herbarium specimens listed in Supplementary Material II, taxonomic treatments in floristic studies (e.g., Clayton & Renvoize, 1982; Gibbs Russell et al., 1990; Shouliang & Phillips, 2006), the descriptions of Clayton et al. (2006), and through analysis of images of type specimens (available at JSTOR Plants). Fifty-eight morphological traits (41 qualitative and 17 quantitative) were recorded for the 49 taxa analyzed. The morphological characters (vegetative and reproductive) were determined according to the methodology described in Peichoto et al. (2008). Quantitative characters were coded by discretizing them with the segment coding method proposed by Chappill (1989), which divides the range of variation into a number of segments proportional to the variability of the character. The list and codification of the 58 characters are shown in Appendix I, while the morphological matrix is presented in Supplementary Material III.

2.4 Phylogenetic analyses

The two matrices, molecular and morphological, were analyzed separately. The molecular matrix including the two plastid markers concatenated (49 taxa \times 2949 base pairs [bp]) was analyzed under a Bayesian approach. Bayesian inference was conducted using BEAST v.1.0.8 (Drummond et al., 2012). The Akaike information criterion (AIC) implemented in jModelTest v.2.1.4 (Darriba et al., 2012) selected GTR+G as the appropriate model of nucleotide substitution. Bayesian analysis was conducted on the molecular data matrix with settings as follows: GTR+G substitution model, with site-rate heterogeneity modeled with four gamma categories and estimated base frequencies. To select the appropriate molecular clock model and the process that best explains our data, we calculated the marginal likelihood of the data under an uncorrelated relaxed log normal clock (URLC) and a strict clock (SC), as well as each of them with pure birth Yule and birth-death priors by the Nested Sample method (Russel et al., 2018) with the software BEAST v.2.6 (Bouckaert et al., 2019), following instructions from the tutorial (Barido-Sottani et al., 2018). We then used the marginal likelihoods to calculate the Bayes factor (BF) (Jeffreys, 1935) for each comparison and interpreted the results according to the standard reported by Kass & Raftery (1995). The results indicated strong support for an uncorrelated relaxed log normal clock with a pure birth Yule prior ($BF_{URLC \text{ vs. } SC} = 7.24$; $BF_{URCL \text{ pure birth vs. URCL birth death}} = 63.61$). After the tests mentioned above, an uncorrelated relaxed clock was used to allow each branch of

our phylogenetic tree to have its own evolutionary rate, meaning that the rate at one branch did not depend upon the rate at any of the neighboring branches (Drummond et al., 2006). The different rates were sampled from a log-normal probability distribution. We used a random starting tree and a pure birth Yule process as tree priors. The Yule process assumes a (unknown) constant lineage birth rate for each branch in the tree. Two independent runs of 10 million generations each were sampled every 1000 generations. To identify when the analyses had reached stationarity, we checked the output files for convergence and effective sample size > 200 with Tracer v.1.6 (Rambaut & Drummond, 2013). Based on this convergence diagnosis, the first 2500 trees sampled were discarded as burn-in from each analysis by using TreeAnnotator v.1.7.1 (Drummond et al., 2012). Trees of the two runs were combined using LogCombiner v.1.8.4 and the maximum credibility tree was displayed in FigTree v.1.3.1 (Rambaut, 2009). Statistical support was determined by assessing the Bayesian posterior probabilities (PP) (Rannala & Yang, 1996).

The morphological matrix, including the same 49 taxa and 58 characters (41 qualitative and 17 quantitative), was analyzed under the parsimony criterion. The parsimony analysis was performed using TNT (Goloboff et al., 2008). Uninformative characters were deactivated. The search strategy consisted of heuristic searches performed using 10 000 series of random addition sequences followed by Tree bisection and reconnection branch rearrangements and retaining two trees per series. The trees found were saved in memory and additionally, tree bisection and reconnection (TBR) swapped, retaining a maximum of 20 000 trees. A strict consensus tree was generated from the most parsimonious trees. To identify putative diagnostic characters for the clade of interest, character optimizations were evaluated. We performed the optimizations in most parsimonious trees obtained, using the command “Common Mapping” of TNT, by which only the optimizations common to all individual trees are represented in the consensus diagram.

3 Results

Seventy-one new sequences from two plastid DNA regions (*ndhF* and *trnL-F*) belonging to the 38 *Schizachyrium* taxa analyzed were generated for the present study. From a total of 2949 bp of the concatenated alignment (*ndhF* and *trnL-F*), 66 bp were phylogenetically informative. The Bayesian tree obtained from the two plastid regions is shown in Fig. 1, in which $PP \geq 0.90$ is indicated. The topology shows *Dichanthium aristatum* as sister to all other representatives of the ingroup. *Schizachyrium delavayi* (Hack.) Bor and *S. jeffreysii* (Hack.) Stapf formed a strongly supported clade ($PP=1$), which is sister to the clade composed of *Cymbopogon citratus* and all representatives of the DASH clade here analyzed (i.e., *Andropogon*, *Schizachyrium*, and *Hyparrhenia* species). The DASH clade ($PP=1$) is formed by two major groups. One of these groups (hereafter named *Schizachyrium* s.s.) is strongly supported ($PP=0.99$) and is formed by 26 *Schizachyrium* taxa, including the type species of the genus, *S. condensatum*. The other group (with low

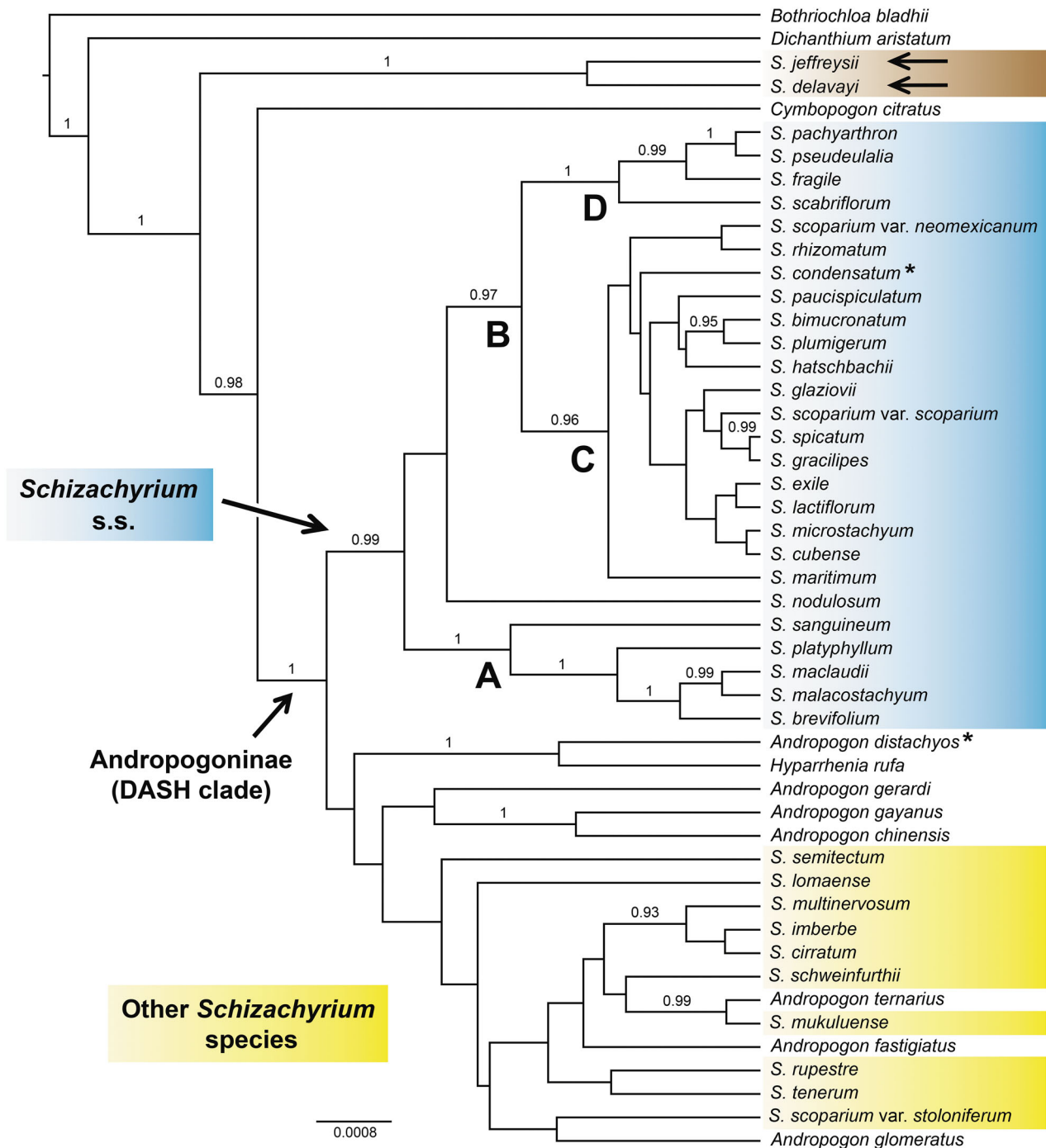


Fig. 1. Maximum clade credibility tree obtained from Bayesian inference analysis of two plastid DNA regions (*ndhF* and *trnL-F*) of *Schizachyrium* and related species. Posterior probabilities (PP) ≥ 0.90 are shown above branches. Main clades and internal clades within *Schizachyrium* s.s. are indicated. The two *Schizachyrium* taxa not related to the remaining species of the genus are marked with arrows. The type species of *Schizachyrium* and *Andropogon* are each marked with an asterisk (*). The scale bar at the bottom indicates the substitutions/site.

support) includes representatives of *Andropogon*, *Hyparrhenia*, and ten species of *Schizachyrium*, here informally named “other *Schizachyrium* species”: *S. cirratum* (Hack.) Nash, *S. imberbe*, *S. lomaense* A. Camus, *S. mukuluense* Vanderyst, *S. multinervosum* Nash, *S. rupestre* (K. Schum.) Stapf, *S. schweinfurthii* (Hack.) Stapf, *S. scoparium* var. *stoloniferum* (Nash) Wipff, *S. semitectum* (Swallen) Reeder, and *S. tenerum* (Fig. 1). Within *Schizachyrium* s.s., two main clades were recovered: clade A (PP=1), with *S. sanguineum* as sister to the clade composed of *S. brevifolium*, *S. maclaudii* (Jacq.-Fél.) S. T. Blake, *S. malacostachyum* (J. Presl) Nash, and *S. platyphyllum* (Franch.) Stapf; and clade B (PP=0.97),

including the remaining *Schizachyrium* s.s. species, distributed in clades C (PP=0.96) and D (PP=1). *Schizachyrium nodulosum* (Hack.) Stapf is sister to clade B.

When we analyzed 41 qualitative morphological characters for the same 49 species, we found that the parsimony analysis tree resulted in a mostly unresolved tree (not shown). However, when 17 quantitative characters were added to the morphological matrix, the parsimony analysis resulted in two mostly resolved trees of 422 steps. The consensus tree is shown in Fig. 2. With respect to the *Schizachyrium* s.s. species, this morphological tree is quite congruent with the molecular one: the same 26

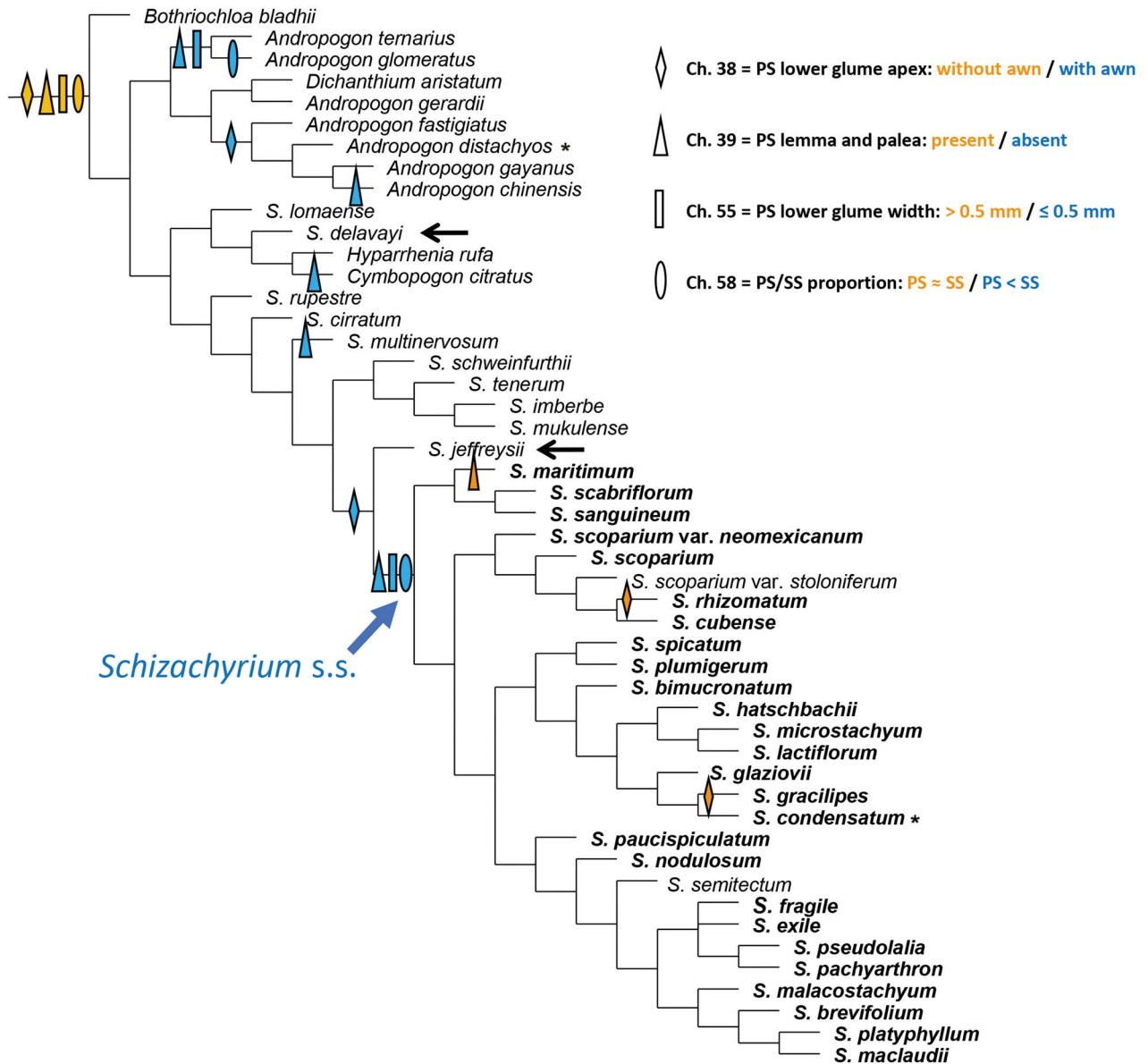


Fig. 2. Strict consensus tree of the two most parsimonious trees obtained from parsimony analysis of morphological data of *Schizachyrium* and related species. The 26 *Schizachyrium* species included in the *Schizachyrium* s.s. clade of molecular analysis are highlighted in bold. The two *Schizachyrium* taxa not related to the remaining species of the genus in the molecular tree are each marked with arrows. The type species of *Schizachyrium* and *Andropogon* are each marked with an asterisk (*). The optimizations of four diagnostic characters are shown. PS, pedicellate spikelet; SS, sessile spikelet.

Schizachyrium species appear forming the *Schizachyrium* s.s. clade, but in this case, it also includes *S. semitectum* and *S. scoparium* var. *stoloniferum*. Other discrepancies in relation to the molecular tree, outside the *Schizachyrium* s.s. clade, are the remaining species of the genus (here called “other *Schizachyrium* species”) not closely related to the *Andropogon* species, *S. jeffreysii* as sister to the *Schizachyrium* s.s. clade, and *S. delavayi* and *S. lomaense* closely related to *Hyparrhenia* and *Cymbopogon* species (Fig. 2).

The optimizations of morphological characters indicated that four (two qualitative and two quantitative) support the *Schizachyrium* s.s. clade (Fig. 2): reduced pedicellate spikelets, shorter than the sessile ones (character [ch.] 58), with lower glume less than or equal to 0.5 mm wide (ch. 55), awned [except *S. gracilipes* (Hack.) A. Camus and *S. rhizomatum* (Swallen) Gould] (ch. 38) and without lemma and palea [except *S. maritimum* (Chapm.) Nash] (ch. 39). The “other *Schizachyrium* species” have pedicellate spikelets similar to the sessile ones, with conspicuous lower glume (wider than 0.5 mm), mucicous (except *S. multinervosum*, with a short awn 1–2 mm long), and generally with lemma and palea.

4 Discussion

We presented here a phylogenetic analysis to circumscribe *Schizachyrium* with the largest sample of the genus to date, including more than 63% of its species, 23 of which had never been included in phylogenetic studies before. Additionally, this is the first phylogenetic analysis to include the type species of the genus, *S. condensatum*, as recently clarified by Welker et al. (2021). The phylogenetic study of Silva et al. (2015) included a *Schizachyrium* specimen (voucher: C. Silva 843, HUEFS) labeled as *S. condensatum*, which actually corresponded to *S. microstachyum*.

Our molecular phylogeny showed that *Schizachyrium* is a non-monophyletic genus, including at least three main lineages: 26 taxa formed a highly supported *Schizachyrium* s.s. clade, including the type species; ten taxa, referred to as “other *Schizachyrium* species”, appeared intermixed to *Andropogon* species with low support; and two other species (*S. delavayi* and *S. jeffreysii*) appeared clearly separated from other representatives of these two genera (Fig. 1). Regarding geographical distribution, from the 26 species of *Schizachyrium* s.s. clade, 17 are American, four from Africa, two from Australia and Asia, one is Australian, and two are of wide distribution. The “other *Schizachyrium* species” include four species from Africa and six from America, while *S. delavayi* is from China and India and *S. jeffreysii* from Africa.

The plastome phylogenomic analysis of Arthan et al. (2017) recovered *Schizachyrium* species in two distinct lineages: one clade with the majority of its species, and another clade, sister to *Andropogon fastigiatus* [\equiv *Diectomis fastigiata* (Sw.) P. Beauv.], formed by *S. imberbe* and *S. tenerum* (both included here in the “other *Schizachyrium* species” group). The plastome study of McAllister et al. (2018) indicated that *Schizachyrium* includes three lineages: one clade comprising most of the species of the genus (*Schizachyrium* s.s. clade) and another composed of some *Schizachyrium* and *Andropogon* species; these authors also recovered *S. delavayi* near

Bothriochloa Kuntze, far away from the other *Schizachyrium* species sampled. The broad phylogenomic analysis of the tribe Andropogoneae performed by Welker et al. (2020) also recovered a similar arrangement regarding *Schizachyrium* taxa, with a clade including most of its species (11) and another clade, sister to *Diectomis fastigiata*, including five species [*S. cirratum*, *S. imberbe*, *S. salzmannii* (Trin. ex Steud.) Nash, *S. tenerum*, and *S. ursulus* Stapf] plus some *Andropogon* species. In addition, *S. thollonii* (Franch.) Stapf was recovered in another clade mostly composed of *Andropogon* species, and *S. delavayi* appears in a position distant from the rest of the *Schizachyrium* taxa, closely related to *Bothriochloa*, *Capillipedium* Stapf, *Dichanthium*, and *Euclasta* Franch. species (Welker et al., 2020).

With a much larger sample of the genus, particularly for American species, our molecular analysis confirmed that *Schizachyrium* contains two distinct main lineages and at least two distant species (see Fig. 1). However, these two main lineages do not correspond to the groups previously defined through typological studies of the inflorescence (Peichoto et al., 2008) and the taxonomic revision of the South American species (Peichoto, 2010) (i.e., taxa with sparsely branched inflorescences and straight rachis internodes and pedicels versus taxa with highly branched inflorescences and flexuous rachis internodes and pedicels). Arthan et al. (2017) proposed that the two main lineages of *Schizachyrium* correspond to the two sections recognized by Clayton (1964) for the genus. They also suggested that these two lineages could be differentiated by the indumentum of the rachis internodes and pedicels, the development of the pedicellate spikelets, and the shape of the upper lemmas. According to these authors, the group formed by *S. imberbe* and *S. tenerum* has glabrous rachis internodes and pedicels, well-developed pedicellate spikelets, and shortly bilobed upper lemmas. In contrast, the taxa of the clade that includes most of the *Schizachyrium* species would share pubescent rachis internodes and pedicels, reduced pedicellate spikelets, and deeply bilobed upper lemmas (Arthan et al., 2017). However, our more extensive analysis showed that the indumentum of the rachis internodes and pedicels, as well as the apex of the upper lemmas, are variable in the *Schizachyrium* s.s. species. The majority of these species have rachis internodes and pedicels with trichomes in marginal lines and deeply bilobed upper lemmas, but *S. brevifolium*, *S. maclaudii*, and *S. platyphyllum* have glabrous rachis internodes and pedicels; and *S. cubense* (Hack.) Nash, *S. exile* (Hochst.) Pilg., *S. maritimum*, *S. scoparium* (Michx.) Nash var. *scoparium*, and *S. scoparium* var. *neomexicanum* (Nash) Hitchc. have shortly bilobed upper lemmas. Our results support that the reduced pedicellate spikelets (i.e., shorter than the sessile ones) characterize the *Schizachyrium* s.s. group determined, as discussed below.

The morphological analysis presented here (including 17 quantitative characters in addition to the commonly used qualitative features) is congruent in relation to the *Schizachyrium* s.s. clade obtained in the molecular analysis: the *Schizachyrium* s.s. clade includes the same 26 species and only two taxa, *S. semitectum* and *S. scoparium* var. *stoloniferum*, appear in this clade in the morphological tree, but not in the molecular analysis. The conflictive positions of these two species should be further investigated using new

samples in the molecular analysis but might be a result of morphological convergence.

The optimizations of morphological characters showed that four features (two qualitative and two quantitative) support the *Schizachyrium* s.s. clade. These four characters refer to the pedicellate spikelets. The two quantitative features (ch. 55: lower glume width of pedicellate spikelets \leq 0.5 mm and ch. 58: pedicellate spikelets shorter than the sessile spikelets) fit perfectly to the *Schizachyrium* s.s. clade in the morphological tree, while the states of the qualitative ones (ch. 38: awned lower glume of pedicellate spikelets; ch. 39: lemma and palea absent in pedicellate spikelets) showed a few exceptions (*S. rhizomatum* and *S. gracilipes* for ch. 38 and *S. maritimum* for ch. 39) (Fig. 2). The development of the pedicellate spikelets is a relevant character supported in previous taxonomic (Peichoto, 2010, p. 305, Welker & Longhi-Wagner, 2012, p. 201) and phylogenomic (Arthan et al., 2017, p. 425) studies. The results obtained here provide three additional characteristics of the pedicellate spikelets (spikelets with narrow lower glumes, awned, and without lemmas and paleas) that can be useful to identify the *Schizachyrium* s.s. clade. The remaining species here referred to as “other *Schizachyrium* species” have well-developed pedicellate spikelets (of a size similar to or slightly lower than that of the sessile spikelets), which are generally muticous and with lemmas and paleas (see Fig. 2).

Within the *Schizachyrium* s.s. clade (Fig. 1), some clades were recovered with strong support. Clade A comprises the annual species *S. brevifolium*, *S. maclaudii*, *S. malacostachyum*, and *S. platyphyllum*, also recovered in our morphological tree. Clade B includes two internal clades: clade D with annual species mainly from Australia [*S. fragile* (R. Br.) A. Camus, *S. pachyarthron* C. A. Gardner, and *S. pseudolalia* (Hosok.) S. T. Blake] and *S. scabriflorum* a perennial, from South America, which have reduced pedicellate spikelets and frequently developed awns (longer than 4 mm), and clade C including mainly perennial species from American (except *S. exile*, annual from Africa and Asia), which have pedicellate spikelet with shorter awns (often less than 4 mm long).

The two morphological groups previously defined by Peichoto et al. (2008) and Peichoto (2010) were partly recovered in the *Schizachyrium* s.s. clade derived from plastid DNA markers. Clades A and D include taxa with sparsely branched inflorescences and straight rachis internodes and pedicels, whereas clade C is formed by species with highly branched inflorescences and flexuous rachis internodes and pedicels, zigzagging at maturity (except *S. paucispiculatum* and *S. scoparium* var. *neomexicanum*, which have straight rachis internodes and pedicels at maturity). Considering that the morphological groups proposed by Peichoto et al. (2008) and Peichoto (2010) were defined from the revision of species of only part of the distribution area (South America), our results, which are based on a more comprehensive analysis, provide new insights on morphological features whose diagnostic value can be evaluated in future studies. However, there are still at least 22 species of *Schizachyrium* that have not yet been included in a DNA sequence study, and these species might not necessarily exhibit the same four apparent synapomorphic characters found in our morphological analysis.

Our phylogenetic analysis corroborates that *Schizachyrium* s.l. is not monophyletic and comprises at least three lineages: 26 of the 38 analyzed species belong to the *Schizachyrium* s.s. clade; of the remaining species, the majority appear related to *Andropogon*, and two, *S. delavayi* and *S. jeffreysii* are not aligned with either genus. Further analysis, with a larger sample of *Schizachyrium* species, is needed to determine their taxonomic alignment. The morphological evidence (including quantitative characters) and the molecular phylogeny were quite congruent with respect to the *Schizachyrium* s.s. clade. Four morphological characters proved to support this clade: (i) reduced pedicellate spikelets (shorter than the sessile ones), with (ii) lower glume less than or equal to 0.5 mm wide, (iii) awned, and (iv) without lemmas and paleas. We propose here these four synapomorphies as diagnostic for *Schizachyrium* s.s. species.

Acknowledgements

We thank the directors and curators of CANB, G, GH, MO, NY, PRE, and US herbaria for the loan of specimens that made this study possible. We also thank FO Zuloaga for critical reading of an early version of the manuscript. Funding of this research was provided by grants from the Secretaría General de Ciencia y Técnica-Universidad Nacional del Nordeste (PI A013-2013, A009-2017), Consejo Nacional de Investigaciones Científicas y Técnicas (PI 11420100100195), and PICTO-UNNE N°199-2011, Argentina. CADW thanks Conselho Nacional de Desenvolvimento Científico e Tecnológico (CNPq, Brazil) for grants and fellowships (426334/2018-3, 150896/2019-0).

References

- Arthan W, McKain MR, Traiperm P, Welker CAD, Teisher JK, Kellogg EA. 2017. Phylogenomics of Andropogoneae (Panicoidae: Poaceae) of mainland Southeast Asia. *Systematic Botany* 42: 418–431.
- Barido-Sottani J, Bošková V, Plessis LD, Kühnert D, Magnus C, Müller V, Müller NF, Pečerska J, Rasmussen DA, Zhang C, Drummond AJ, Heath TA, Pybus OG, Vaughan TG, Stadler T. 2018. Taming the BEAST—A community teaching material resource for BEAST 2. *Systematic Biology* 67: 170–174.
- Bouchenak-Khelladi Y, Salamin N, Savolainen V, Forest F, Van Der Bank M, Chase MW, Hodkinson TR. 2008. Large multi-gene phylogenetic trees of the grasses (Poaceae): Progress towards complete tribal and generic level sampling. *Molecular Phylogenetics and Evolution* 47: 488–505.
- Bouchenak-Khelladi Y, Verboom GA, Hodkinson TR, Salamin N, Francois O, Ni Chonghaile G, Savolainen V. 2009. The origins and diversification of C₄ grasses and savanna-adapted ungulates. *Global Change Biology* 15: 2397–2417.
- Bouchenak-Khelladi Y, Slingsby JA, Verboom GA, Bond WJ. 2014. Diversification of C₄ grasses (Poaceae) does not coincide with their ecological dominance. *American Journal of Botany* 101: 300–307.
- Bouckaert R, Vaughan TG, Barido-Sottani J, Duchêne S, Fourment M, Gavryushkina A, Heled J, Jones G, Kühnert D, De Maio N, Matschiner M, Mendes FK, Müller NF, Ogilvie HA, du Plessis L, Poppinga A, Rambaut A, Rasmussen D, Siveroni I, Suchard MA,

- Wu CH, Xie D, Zhang C, Stadler T, Drummond AJ. 2019. BEAST 2.5: An advanced software platform for Bayesian evolutionary analysis. *PLoS Computational Biology* 15: e1006650.
- Chappill JA. 1989. Quantitative characters in phylogenetic analysis. *Cladistics* 5: 217–234.
- Clayton WD. 1964. Studies in the Gramineae: V. *Kew Bulletin* 17: 465–470.
- Clayton WD, Renvoise SA. 1982. Gramineae (Part 3). In: Polhill RM ed. *Flora of Tropical East Africa*. Rotterdam: A. A. Balkema. 451–898.
- Clayton WD, Renvoise SA. 1986. *Genera Graminum*. London: Her Majesty's Stationery Office.
- Clayton WD, Vorontsova MS, Harman KT, Williamson H. 2006 (onwards). GrassBase—The online world grass flora [online]. Available from <http://www.kew.org/data/grasses-db.html> [accessed 16 January 2020].
- Darriba D, Taboada GL, Doallo R, Posada D. 2012. jModelTest 2: More models, new heuristics and parallel computing. *Nature Methods* 9: 772.
- Doyle JJ, Doyle JL. 1987. A rapid DNA isolation procedure for small quantities of fresh leaf tissue. *Phytochemical Bulletin* 19: 11–15.
- Drummond AJ, Ho SYW, Phillips MJ, Rambaut A. 2006. Relaxed phylogenetics and dating with confidence. *PLoS Biology* 4(5): e88.
- Drummond AJ, Suchard MA, Xie D, Rambaut A. 2012. Bayesian phylogenetics with BEAUti and the BEAST 1.7. *Molecular Biology and Evolution* 29: 1969–1973.
- Estep MC, McKain MR, Vela Diaz D, Zhong J, Hodge JG, Hodkinson TR, Layton DJ, Malcomber ST, Pasquet R, Kellogg EA. 2014. Allopolyploidy, diversification, and the Miocene grassland expansion. *Proceedings of the National Academy of Sciences of the United States of America* 111: 15149–15154.
- Gibbs Russell GE, Watson L, Koekemoer M, Smook L, Barker NP, Anderson HM, Dallwitz MJ. 1990. *Grasses of Southern Africa*. Memoirs of the Botanical Survey of South Africa 58. Pretoria: National Botanic Gardens, Botanical Research Institute.
- Goloboff PA, Farris JS, Nixon KC. 2008. TNT, a free program for phylogenetic analysis. *Cladistics* 24: 774–786.
- Hackel J, Vorontsova MS, Nanjarisoa OP, Hall RC, Razanatsoa J, Malakasi P, Besnard G. 2018. Grass diversification in Madagascar: in situ radiation of two large C₃ shade clades and support for a Miocene to Pliocene origin of C₄ grassy biomes. *Journal of Biogeography* 45: 750–761.
- Hall TA. 1999. BioEdit: a user-friendly biological sequence alignment editor and analysis program for Windows 95/98/NT. *Nucleic Acids Symposium Series* 41: 95–98.
- Jeffreys H. 1935. Some test of significance, treated by the Theory of Probability. *Proceedings of the Cambridge Philosophy Society* 31: 203–222.
- Kass RE, Raftery AE. 1995. Bayes factors. *Journal of the American Statistical Association* 90: 773–795.
- Mathews S, Spangler RE, Mason-Gamer RJ, Kellogg EA. 2002. Phylogeny of Andropogoneae inferred from phytochrome B, GBSSI, and ndhF. *International Journal of Plant Sciences* 163: 441–450.
- McAllister CA, McKain MR, Li M, Bookout B, Kellogg EA. 2018. Specimen-based analysis of morphology and the environment in ecologically dominant grasses: the power of the herbarium. *Philosophical Transactions of the Royal Society B: Biological Sciences* 374: 20170403.
- Nicora EG, Rúgolo de Agrasar ZE. 1987. *Los géneros de Gramineas de América Austral*. Buenos Aires: Ed. Hemisferio Sur.
- Olmstead R, Sweere JA. 1994. Combining data in phylogenetic systematics: an empirical approach using three molecular data sets in the Solanaceae. *Systematic Biology* 43: 467–481.
- Peichoto MC. 2010. Revisión taxonómica de las especies del género *Schizachyrium* (Poaceae: Andropogoneae) de Sudamérica. *Candollea* 65: 301–345.
- Peichoto MC, Mazza SM, Solís Neffa VG. 2008. Morphometric analysis of *Schizachyrium condensatum* (Poaceae) and related species. *Plant Systematics and Evolution* 276: 177–189.
- Preston JC, Wang H, Kursel L, Doebley J, Kellogg EA. 2012. The role of *teosinte glume architecture (tga1)* in coordinated regulation and evolution of grass glumes and inflorescence axes. *New Phytologist* 193: 204–215.
- Rambaut A. 2009. FigTree version 1.3.1 [computer program] [online]. Available from <http://tree.bio.ed.ac.uk> [accessed 16 January 2020].
- Rambaut A, Drummond AJ. 2013. Tracer version 1.6 [computer program and documentation distributed by the author] [online]. Available from <http://beast.bio.ed.ac.uk/Tracer> [accessed 16 January 2020].
- Rannala B, Yang Z. 1996. Probability distribution of molecular evolutionary trees: a new method of phylogenetic inference. *Journal of Molecular Evolution* 43: 304–311.
- Russel PM, Brewer BJ, Klaere S, Bouckaert RR. 2018. Model selection and parameter inference in phylogenetics using Nested Sampling. *Systematic Biology* 68: 219–233.
- Shouliang C, Phillips SM. 2006. *Schizachyrium*, *Cymbopogon*, *Hyparrhenia*. In: Wu ZY, Raven PH, Hong DY eds. *Flora of China*. Beijing: Science Press; St. Louis: Missouri Botanical Garden Press. 22: 621–633.
- Silva C, Snak C, Schnadelbach AS, van den Berg C, Oliveira RP. 2015. Phylogenetic relationships of *Echinoalaena* and *Ichnanthus* within Panicoideae (Poaceae) reveal two new genera of tropical grasses. *Molecular Phylogenetics and Evolution* 93: 212–233.
- Skendzic EM, Columbus JT, Cerros-Tlatilpa R. 2007. Phylogenetics of Andropogoneae (Poaceae: Panicoideae) based on nuclear ribosomal internal transcribed spacer and chloroplast *trnL-F* sequences. *Aliso* 23: 530–544.
- Soreng RJ, Peterson PM, Romaschenko K, Davidse G, Zuloaga FO, Judziewicz EJ, Filgueiras TS, Davis JI, Morrone O. 2015. A worldwide phylogenetic classification of the Poaceae. *Journal of Systematics and Evolution* 53: 117–137.
- Soreng RJ, Peterson PM, Romaschenko K, Davidse G, Teisher JK, Clark LG, Barberá P, Gillespie LJ, Zuloaga FO. 2017. A worldwide phylogenetic classification of the Poaceae (Gramineae) II: an update and a comparison of two 2015 classifications. *Journal of Systematics and Evolution* 55: 259–290.
- Spangler R, Zaitchik B, Russo E, Kellogg EA. 1999. Andropogoneae evolution and generic limits in *Sorghum* (Poaceae) using *ndhF* sequences. *Systematic Botany* 24: 267–281.
- Taberlet P, Gielly L, Pautou G, Bouvet J. 1991. Universal primers for amplification of three non-coding regions of chloroplast DNA. *Plant Molecular Biology* 17: 1105–1109.
- Thiers B. 2020 (continuously updated). Index Herbariorum: A global directory of public herbaria and associated staff. New York Botanical Garden's Virtual Herbarium, New York [online]. Available from <http://sweetgum.nybg.org/science/ih/> [accessed 16 January 2020].
- Teerawatananon A, Jacobs SWL, Hodkinson TR. 2011. Phylogenetics of Panicoideae (Poaceae) based on chloroplast and nuclear DNA sequences. *Telopea* 13: 115–142.

- Türpe AM. 1984. Revision of the South American species of *Schizachyrium* (Gramineae). *Kew Bulletin* 39: 169–178.
- Watson L, Dallwitz MJ. 1992. *The grass genera of the world*. Wallingford: CAB International.
- Welker CAD, Longhi-Wagner HM. 2012. Sinopse do gênero *Schizachyrium* Nees (Poaceae—Andropogoneae) no estado do Rio Grande do Sul, Brasil. *Iheringia, Série Botânica* 67: 199–223.
- Welker CAD, McKain MR, Estep MC, Pasquet RS, Chipabika G, Pallangyo B, Kellogg EA. 2020. Phylogenomics enables biogeographic analysis and a new subtribal classification of Andropogoneae (Poaceae—Panicoideae). *Journal of Systematics and Evolution* 58: 1003–1030.
- Welker CAD, Prado J, Kellogg EA, Gandhi KN. 2021. Clarifying the type of the polyphyletic genus *Schizachyrium* (Poaceae: Andropogoneae). *Kew Bulletin*. <https://doi.org/10.1007/S12225-021-09939-2>.
- Zanin A, Longhi-Wagner HM. 2011. Revisão de *Andropogon* (Poaceae—Andropogoneae) para o Brasil. *Rodriguésia* 62: 171–202.
- Zannin A, Viana PL, Welker CAD, Filgueiras TS. 2019. *Andropogon saxicola* (Poaceae: Andropogoneae), a new species from Brazil. *Phytotaxa* 397: 83–90.

Supplementary Material

The following supplementary material is available online for this article at <http://onlinelibrary.wiley.com/doi/10.1111/jse.12807/supinfo>:

Supplementary material I. Molecular matrix showing *ndhF* and *trnL-F* sequences concatenated in the 49 taxa analyzed.

Supplementary material II. Details of the specimens examined for the morphological analysis.

Supplementary material III. Morphological matrix showing the character states of the 58 characters analyzed in the 49 taxa examined.

Appendix I. Character codification and character states used in the morphological analyses of *Schizachyrium* and related taxa. PS, pedicellate spikelet; SS, sessile spikelet.

Character	States or ranges
Qualitative characters	
Ch. 1. Habit	0 (annual), 1 (perennial)
Ch. 2. Basal portion of the culm	0 (robust), 1 (delicate)
Ch. 3. Form of growth of the culm in the proximal region	0 (erect), 1 (slightly geniculate), 2 (decumbent)
Ch. 4. Rhizomes	0 (absent), 1 (present: from short to developed)
Ch. 5. Arrangement of floriferous branches	0 (concentrated in the distal portion of the culm), 1 (in the middle and distal portion of the culm)
Ch. 6. Indumentum of the leaf sheath	0 (glabrous), 1 (with trichomes)
Ch. 7. Blade section	0 (flat or conduplicate), 1 (involute)
Ch. 8. Blade apex	0 (acute), 1 (obtuse or subobtuse)
Ch. 9. Ligule shape	0 (truncate), 1 (obtuse or oblique)

Continued

Character	States or ranges
Ch. 10. Ligule pilosity	0 (glabrous), 1 (ciliate)
Ch. 11. Indumentum of the basal portion of the blade	0 (glabrous), 1 (with trichomes)
Ch. 12. Shape of the basal portion of the blade	0 (without a basal narrowing), 1 (with a basal narrowing)
Ch. 13. Inflorescence shape	0 (panicle-like form, with lax to dense branches), 1 (corymb-like form), 2 (digitate or fascicled in the apex of the culm)
Ch. 14. Number of racemes per spatheole	0 (1 raceme), 1 (2 or more racemes)
Ch. 15. Peduncle position at maturity	0 (included in the spatheole), 1 (apical portion visible, up to 1/3 of its length visible at the apex of the spatheole), 2 (apical and medium portion visible, 1/3 to 2/3 of its length visible at the apex of the spatheole)
Ch. 16. Spatheole shape	0 (convolute), 1 (subconvolute), 2 (open)
Ch. 17. Spikelet types along the raceme*	0 (heterogamous spikelets along the raceme), 1 (homogamous spikelets in the basal and/or apical portion of the raceme)
Ch. 18. Number of pairs of spikelets in the raceme	0 (<10 pairs), 1 (>10 pairs)
Ch. 19. Rachis internode disposition at maturity	0 (flexuous), 1 (straight)
Ch. 20. Rachis internode shape	0 (filiform), 1 (notoriously dilated), 2 (expanded at the apex and narrow at the base)
Ch. 21. Rachis internode indumentum	0 (glabrous), 1 (with trichomes in 1–3 marginal lines), 2 (with trichomes in oblique line), 3 (with trichomes on the surface, not in lines)
Ch. 22. Callus indumentum	0 (glabrous or shortly pilose, with very short trichomes), 1 (conspicuously pilose)
Ch. 23. Spikelet disposition at maturity	0 (appressed or subappressed), 1 (divergent)
Ch. 24. Spikelet shape*	0 (homomorphic), 1 (dimorphic), 2 (homomorphic and dimorphic)
Ch. 25. SS sexuality	0 (hermaphrodite), 1 (male), 2 (female)
Ch. 26. SS back of lower glume	0 (flat or slightly concave or convex), 1 (convex or conspicuously convex), 2 (concave or with medium groove)

Continued

Character	States or ranges
Ch. 27. SS lower glume indumentum	0 (glabrous), 1 (pilose)
Ch. 28. SS lower glume consistency	0 (papyraceous or carthaceous), 1 (cartilaginous), 2 (coriaceous)
Ch. 29. SS dorsal surface of lower glume	0 (smooth), 1 (with asperities), 2 (tuberculated-scabrous)
Ch. 30. SS visibility of nerves of the lower glume	0 (nerves not visible), 1 (2-4 visible nerves), 2 (more than 4 visible nerves)
Ch. 31. SS lower glume apex	0 (obtuse or subobtuse), 1 (acute)
Ch. 32. SS shape of lower glume apex	0 (whole), 1 (2-denticulate), 2 (2-mucronate)
Ch. 33. SS wings at lower glume apex	0 (absent), 1 (present)
Ch. 34. SS upper lemma apex	0 (whole, acute or obtuse), 1 (shortly bilobed), 2 (deeply bilobed)
Ch. 35. SS awn of the upper lemma	0 (absent), 1 (present)
Ch. 36. SS palea	0 (absent), 1 (present)
Ch. 37. PS sexuality	0 (neuter), 1 (hermaphrodite), 2 (male), 3 (female)
Ch. 38. PS lower glume apex	0 (without awn), 1 (with awn)
Ch. 39. PS lemma and palea	0 (absent), 1 (present)
Ch. 40. PS pedicel indumentum	0 (glabrous), 1 (with trichomes in 1 line), 2 (with trichomes in 2-3 lines), 3 (with trichomes on the surface, not in lines)
Ch. 41. PS pedicel shape	0 (dorsiventrally compressed), 1 (terete, clavate)

Continued

Character	States or ranges
Discretized quantitative characters	
Ch. 42. Plant height	0 (<75 cm), 1 (75–150 cm), 2 (>150 cm)
Ch. 43. Blade width	0 (<2 mm), 1 (2–5 mm), 2 (>5 mm)
Ch. 44. Blade length	0 (<150 mm), 1 (150–300 mm), 2 (>300 mm)
Ch. 45. Ligule length	0 (<1.5 mm), 1 (1.5–3 mm), 2 (>3 mm)
Ch. 46. Inflorescence number of racemes per culm	0 (up to 4(-6) racemes), 1 (7 to 20 racemes), 2 (21 to 50 racemes), 3 (more than 50 racemes)
Ch. 47. Peduncle length	0 (<10 mm), 1 (10–20 mm), 2 (>20 mm)
Ch. 48. Spatheole length	0 (<50 mm), 1 (50–100 mm), 2 (>100 mm)
Ch. 49. Raceme length	0 (<50 mm), 1 (50–100 mm), 2 (>100 mm)
Ch. 50. Rachis internode length	0 (<3 mm), 1 (3–6 mm), 2 (>6 mm)
Ch. 51. SS lower glume length	0 (<5.5 mm), 1 (5.5–8 mm), 2 (>8 mm)
Ch. 52. SS lower glume width	0 (<0.5 mm), 1 (0.5–1 mm), 2 (>1 mm)
Ch. 53. SS awn length of the upper lemma	0 (<10 mm), 1 (10–20 mm), 2 (>20 mm)
Ch. 54. PS lower glume length	0 (<3 mm), 1 (3–6 mm), 2 (>6 mm)
Ch. 55. PS lower glume width	0 (≤0.5 mm), 1 (>0.5 mm)
Ch. 56. PS awn length	0 (<1 mm), 1 (1–4 mm), 2 (4–10 mm), 3 (>10 mm)
Ch. 57. PS pedicel length	0 (<4 mm), 1 (>4 mm)
Ch. 58. PS/SS proportion	0 (PS ≈ SS), 1 (PS < SS)

*According to Nicora & Rúgolo de Agrasar (1987, p. 584).